Article

Exploring the Influencing Factors and Formation of the Blind Zone of a Semitrailer Truck in a Right-Turn Collision

Qingzhou Wang [1], Jiarong Sun [1], Nannan Wang [1], Yu Wang [1], Yang Song [2] and Xia Li [1],*

[1] School of Civil and Transportation Engineering, Hebei University of Technology, Tianjin 300401, China
[2] Hebei Key Laboratory of Geotechnical Engineering Safety and Deformation Control, Hebei University of Water Resources and Electric Engineering, Cangzhou 061001, China
* Correspondence: 2006088@hebut.edu.cn

Abstract: The blind zone that accompanies the right-turn process of semitrailer trucks is a major cause of crashes and the high fatality of vulnerable road users (VRUs). Understanding the relationship between the blind zone and right-turn collisions will play a positive role in preventing such accidents. The purpose of this study was to investigate the formation of right-turn blind zones for semitrailer trucks and to determine the factors (turning speed, turning radius, and collision position) influencing the severity of accidents through real-world vehicle tests and PC-CRASH simulation. The results show that the calculation model of the inner wheel difference blind zone established for semitrailer trucks can provide more accurate estimation than the model for rigid trucks, due to the consideration of a virtual third axle between the tractor and the trailer. On the other hand, the PC-CRASH simulation test indicates the turning speed and turning radius directly affect the scale of the inner wheel difference blind zone, and larger blind zone and encroachment on adjacent lanes increase the potential for collision. Moreover, the difference in collision position is closely related to whether the rider suffers a secondary crush. Front position is more likely to cause the cyclist to be crushed. For further analysis, the long-term interaction between the blind zones resulting from the right rearview mirror and the inner wheel difference also increases the risk during a right turn. Therefore, reducing the blind zone in the right-turn process is the key to improving right-turn safety for semitrailer trucks and VRUs.

Keywords: traffic safety; blind zone; semitrailer truck; collision accident; PC-CRASH

1. Introduction

Two-wheeled riders and trucks are important in transportation systems worldwide. However, their routes often cross on limited urban roads [1,2], which results in a road safety issue of increasing public concern. Consequently, many people are killed in accidents related to trucks annually, especially VRUs (pedestrians, bicyclists, motorcycle riders, etc.), who are often injured or even fatally threatened in traffic crashes due to lack of adequate protection. Right-turn collision is a common type of truck—VRU collision between a right-turning truck at an intersection and a non-motorized vehicle or pedestrian moving straight with the right-hand driving rule. It is worth noting that the frequency and lethality of such collisions are extremely high [3,4]. Blind zones are considered to be the critical trigger for accidents and cause serious casualties [5,6]. A European survey showed that 45% of all fatal crashes between bicycles and trucks are caused by cyclists in blind zones [7]. Meanwhile, in China, it was found that imperfect truck structural design, including the blind zone of driver's right-turn line of sight and other factors, leads trucks to scratch or crush VRUs when turning right, accounting for about 30% of truck accidents [8]. The driver obtains road information through direct vision (front windows) and indirect vision (rearview mirrors) during the turning process [9,10]. However, due to the restrictions of the vehicle structure, there are many blind zones for the drivers around the truck [11]. The blind zones of the

left and right rearview mirrors are caused by the driver's inability to observe through the rearview mirrors [12]. In the case of a right turn, the blind zone of the rearview mirror is further enlarged, which has an adverse effect on the driver's observation of the surrounding conditions [13]. At the same time, the driver tends to ignore the approaching VRU in the blind zone of the rearview mirror, which may lead to a right-turn collision [10]. The blind zone caused by inner wheel difference is a unique type that accompanies the vehicle turning process. There is a difference in turning radius between the right front wheel and the right rear wheel (for a semitrailer truck, the right front wheel of the tractor and the right rear wheel of the trailer) when the vehicle is turning right, resulting in different paths for two wheels to complete the turn. This radius difference between the front and rear wheels is defined as the "inner wheel difference", and the area swept by the inner wheel difference during the right turn is called the "inner wheel difference blind zone", which is not visible to the driver in the optical rearview mirror. Therefore, once the VRU is within the inner wheel difference blind zone, they are facing a serious risk of being crushed [2]. The blind zone of the inner wheel difference is the main cause of right-turn collisions that threaten the safety of VRUs, and accident data show that more than 70% of accidents were associated with inner wheel difference blind zones, with a fatality rate of over 90% [4]. This problem is more serious for semitrailer trucks with longer bodies and more complex structures, which have larger blind zone areas [14]. Specifically, the following performance of the trailer to the tractor is poor, as the trailer produces a large offset relative to the tractor part when turning right, which further increases the inner wheel difference blind zone and blocks the view of the right rearview mirror due to the trailer body. These factors certainly cause great risk of potential accidents.

Currently, the topic of right-turning trucks colliding with VRUs is appearing more frequently in the literature [2,11,15], but little attention has been given to semitrailer trucks, whose articulated construction complicates their blind zone formation and increases the risk of collisions. Understanding the formation mechanism and influencing factors of the blind zones during the right turn of a semitrailer will play a positive role in preventing crashes. In this paper, to investigate the right-turn situation of a semitrailer, we adopted a hybrid modeling approach involving a real-world vehicle test and PC-CRASH simulation to analyze the formation mechanism of the blind zone of the right rearview mirror during the right turn. The paper proposes an inner wheel difference calculation model applicable to articulated vehicles and measuring the effects of vehicle speed and turning radius on blind zones, as well as the effects of collision positions on the severity of an accident. In addition, it was found that the inner wheel difference blind zone and the right rearview mirror blind zone will produce a certain degree of overlap during a right turn, that is, the "double-blind zone" occurs. Prevention measures considering the double-blind zone were also proposed.

2. Literature Review

The safety issues for trucks and VRUs continue to attract the attention of transportation managers and researchers. Existing studies have investigated the safety of bicycle riding and truck driving by evaluating a variety of topics, including accident causes, accident severity, crash reproduction simulation, and accident prevention and warning [4,5,15,16]. The causes of right-turn collisions and associated risk factors have been investigated to reduce collision.

Truck–VRU right-turn collision has multiple causes. These include misperception and improper operation of the driver [3], VRU lack awareness of blind zones [11], limited visibility due to the vehicle's construction [5], and unsafe road facility layouts [1]. Blind zones continues to be a concern. Studies have concluded that the size of the blind zone is closely related to the height of the driver's eye point above the ground. The results indicated that vehicles with a higher cab were more likely to ignore riders on the vehicle's side, which presents a potential hazard for turning operations [13]. However, the blind zone changes dynamically during vehicle turns, and it would be interesting to know how the

driver's visual range changes during a right turn. In addition, some studies have focused on the blind zone caused by inner wheel difference, whose danger is more apparent during right turns (for right-hand driving situations). The size of the inner wheel difference blind zone is correlated with vehicle wheelbase and length, which means that larger vehicles have a larger blind zone area and higher risk [17]. Effectively solving the problem of inner wheel difference blind zone can contribute to reducing the occurrence of malignant right-turn crashes. Therefore, calculation of the inner wheel difference is the key to obtaining accurate warnings. Zhang et al. [17] established a kinematic model for heavy trucks under low- and medium-speed conditions based on the Ackermann steering principle and established a method to evaluate the inner wheel difference. Zhang et al. [4] established a calculation model with the inner front wheel angle as a variable. By measuring the actual inner front wheel rotation angle, the inner wheel difference can be accurately calculated, and the danger zone can be determined and analyzed. Although these models can obtain the region of inner wheel difference more accurately, they are all based on rigid trucks. Semitrailer trucks differ in their construction, and the articulated structure complicates the calculation of the inner wheel difference. Tsai and Sung [14] proposed an algebraic analytical method for deriving the inner wheel difference of semitrailers, and equations were established based on the vehicle dimensions and steering conditions. This method can predict the steering trajectory of the vehicle almost in real time, but it involves numerous parameters and a complex computational process. Wang et al. [18] modeled the inner wheel difference based on the relationship between the angular velocity and velocity of the wheels during turning, but the inner wheel difference of the trailer part was determined based on the calculation results for the tractor. These studies provide references for the calculation of inner wheel differences in articulated vehicles, but simple and accurate calculation models still need further research.

Additionally, the risk level of collisions has been investigated by many researchers. Vehicle speed, vehicle trajectory, and collision position were found to be influencing factors [19]. Warner et al. [20] reported that the most fatal and serious crashes were significantly affected by increasing speed limits. A higher vehicle speed implies a higher accident severity. Moreover, the vehicle trajectory during a turn is closely related to the turning speed. In particularly, for large vehicles, change in the turning radius affects the scale of the blind zone from the inner wheel difference. A small turning radius leads to a large inner wheel difference and increases the probability of accident risk [21]. In addition, the collision position is considered to be a factor influencing the accident risk level. According to Talbot et al. [5] and Niewoehner and Berg [11], riders are more likely to be crushed and fatally injured by trucks when the initial point of collision is close to the cab. Evaluation of the impacts of these risk factors on the hazard level of an accident is usually accomplished using a large amount of statistical data, but the process of data collection is characterized by long lead times and large errors. Therefore, model-based simulation methods have become widely used technical tools to explore the degree of influence of risk factors on crashes and summarize crash patterns. PC-CRASH can simulate the complete crash process with high resolution [22]. In addition, it can make more accurate predictions of dynamic response processes such as the motion trajectories of accident participants [23–26]. For example, Wei et al. [15] simulated the dynamic response process of rigid truck–electric bicycle collision and crushing under different condition settings based on the established multirigid model, and the difference in the process indicates the accident regular pattern. Yang et al. [27] obtained the wheel trajectory information by PC-CRASH. Through setting appropriate initial conditions, the simulation can effectively reflect the motion trajectory of the accident vehicle. According to previous studies, accident simulation of semitrailer trucks is rarely addressed. Additionally, studies that combine right-turn blind zones with accident hazards are relatively rare.

The aforementioned research indicates that although the inner wheel difference issue during right turns of trucks has attracted attention, the calculation of the inner wheel difference is mostly obtained through the established theoretical model. In addition, the

evaluation criteria for collision risk only focus on the accident rate and damage situation. It should be noted that the blind zone of inner wheel difference is also the main reason for the high casualty in such crashes, and it is necessary to evaluate the crash risk from this perspective. With a focus on the safety of the interaction between a semitrailer truck and a VRU, the main contributions of this study are summarized as follows. A real-vehicle test was utilized to analyze the formation of the blind zone from right-turn inner wheel difference, and a blind zone calculation model was established. At the same time, the influence of turning speed, turning radii, and other factors on the blind zone of a semitrailer truck and the influence of the collision position on injury severity were examined through simulations. In particular, the joint interaction between the blind zone of the right rearview mirror and the blind zone from the inner wheel difference during the turning process was explored. The rest of this paper is organized as follows. Section 3 describes the experimental method and experimental design. Section 4 presents the results and comparisons. Section 5 discusses the interaction mechanism of the double-blind zone. Prevention and control measures are also proposed. Section 6 summarizes and addresses future research.

3. Method

3.1. Accident Statistics

To find collision patterns, 150 traffic accidents that occurred between a right-turning semitrailer truck and a VRU were obtained from 2018–2020. To clarify the collision position, the semitrailer was divided into 5 equidistant areas, numbered 1–5 from the front to the rear of the vehicle, representing 5 different collision positions, as shown in Figure 1. Accident information was obtained from news reports and other materials on the internet. We verified and obtained detailed information about the accidents through telephone interviews and other methods, including the accident time, location, object type, and collision position, which were organized and recorded in a table (Appendix A).
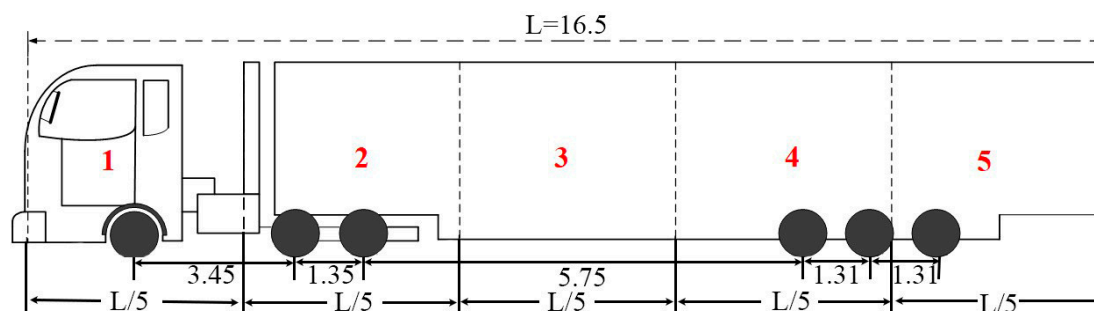

Figure 1. Parameters of the test vehicle (Unit: meters).

3.2. Real-World Test of a Blind Zone

A parking lot was selected, according to the standard two-way four-lane intersection size, to establish a mock right-turn intersection [28]. The Jiefang (CA4250P66K24T1E5) tractor and Brilliant Pengda (HPD9402CCY) trailer that were used as the six-axle semitrailer truck are shown in Figure 1. To establish the plane coordinate system, the trailer's left rear side of the outermost outline of the projection point on the ground was selected as the origin of the coordinate system O, while the forward direction of semitrailer was defined as the positive direction of the Y-axes, and vertical direction was defined as that of the X-axes. From the O point, two tape strips represented X- and Y-axes to record the vehicle right-turn process of different axle of wheel track coordinates.

Two test scenarios were examined. One of the blind zone tests was designed for the inner wheel difference. The semitrailer started from the origin O of the coordinate system, traveled at a speed of 20 km/h and took a right turn at 90°. In order to obtain the maximum blind zone range, the driver maintained the largest steering wheel turning angle for right-turn operation. The semitrailer was not allowed to stop, while a researcher used lime powder to continuously mark the wheel tracks of the first and sixth axles on the

right side to obtain the inner wheel difference blind zone, as shown in Figure 2. The other blind zone test was conducted for the rearview mirror. The simulated turning test measured the turning angle through frequent stops, as shown in Figure 3. The test vehicle started from the origin O and stopped every 15°, and the boundary of the right rearview mirror's visual zone was recorded. Before starting the test, the coordinates of the trajectory of the right wheel of the sixth axle of the semitrailer in the inner wheel difference blind zone test were measured as a reference to determine the parking spot (PS). The starting and ending positions were selected to make a vertical line to intersect at a point, and marked PS was built every 15° at the intersection. The truck stopped at each PS, and the boundary of the visible zone of the right rearview mirror was measured. The truck completed the right turn and stopped the test after the body was straightened. The boundary of the visible zone of the right rearview mirror was determined by the laser-projection method, with laser emission equipment placed at the driver's eye point position. A red laser beam was transmitted to the boundary of the rearview mirror as the tester moved around the projection point of the laser beam on the ground. Simultaneously, the maximum view of the tester for the driver from the rearview mirror was marked on the ground with pylons, and the coordinates were measured and recorded. The entire test process is illustrated in Figure 4.

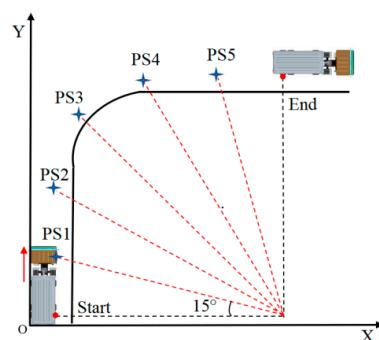**Figure 2.** Blind zone test for the inner wheel difference.

Figure 3. Blind zone test for the rearview mirror.

Figure 4. View boundary measurement for the rearview mirror: (**a**) The semitrailer truck starts to turn, and the rearview mirror has a maximum view; (**b**) the view in the rearview mirror gradually decreases; (**c**) the view of the rearview mirror reaches its minimum value during the turning process, and the rearview mirror fails considerably.

3.3. PC-CRASH Simulation

3.3.1. Accident Reconstruction

In this section, the PC-CRASH accident reproduction model of a right-turning semi-trailer truck and a two-wheeled vehicle collision was established based on the multirigid body theory and a real traffic accident in Tianjin, China. The road is a two-way four-lane road, and the intersection parameters were set with reference to the "Code for design of urban road engineering" [28], according to which the width of the motorway is 3.5 m, the width of the non-motorway is 2.5 m, and the intersection radius is 15 m (Figure 5a). The semitrailer truck described in Section 3.2 was utilized for the simulation, and the technical parameters are shown in Table 1; the size of the two-wheeled vehicle was 1500 × 450 × 1010 mm. To improve the simulation accuracy and adaptability of the simulated reproduced accident, the human dimensions of the 90th percentile of Chinese male adults were selected according to the current national standards [29,30]. A human model with height of 175 cm and weight of 71 kg was used in the simulation process. Therefore, a simulation model of a right-turn collision between a semitrailer truck and a two-wheeled vehicle was established, as shown in Figure 5b. The simulation model rebuilt the real crash through similar crash scenarios in terms of collision points, vehicle speed, damage parts, and bicycle dragging marks. Because the simulation results were consistent with the actual crash, the simulation was believed to reflect the actual collision process. Thus, the analysis of factors influencing the severity of right-turn collisions could be further studied.
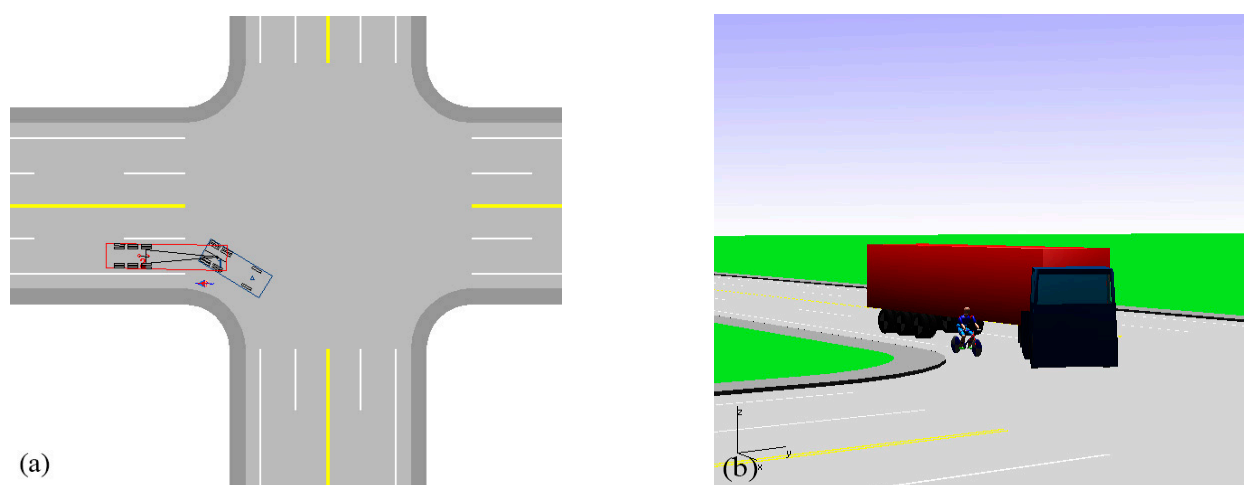

(a)

(b)

Figure 5. Right-turn collision scenario model: (**a**) 2D view of the collision scene; (**b**) 3D view of the collision scene.

Table 1. Technical parameters of the tractor and trailer.

Parameter	Tractor	Trailer	Parameter	Tractor	Trailer
Length/mm	7050	13,000	Width/mm	2500	2500
Height/mm	3560	3400	Total Permissible Weight/kg	25,000	40,000
Wheelbase/mm	3450 + 1350	5750 + 1310 + 1310	Curb Weight/kg	8805	6200
Number of Axles	3	3	Number of Tires	10	12
Front Suspension and Rear Suspension/mm	1470/780	-/1730	Front Tread/mm	2020	-
Rear Tread/mm	1830/1830	1840/1840/1840	Axle Load	7000/18,000	-/24,000

3.3.2. Experimental Design

Generally, the accident severity of right-turn collisions is affected by the turning speed, turning radius (angle), collision position, and the extent of dragging [5,6,17,19]. In this study, the size of the blind zone from the inner wheel difference was defined and

correlated with the probability of collision, which is influenced by the change in the turning parameters; furthermore, the collision position is also closely related to the probability of a secondary crash, which will produce different degrees of accident risk. Therefore, two tests were conducted. One was the blind zone parameter test for the inner wheel difference, and the other was a simulation test for accident severity due to collision position.

(1)   Test to determine the factors influencing the blind zone from the inner wheel difference.

As the driving trajectory of the truck and the inner wheel difference blind zone are affected by the turning speed, various speeds were selected in the simulation to examine their influence on the range of the blind zone caused by the inner wheel difference. According to a survey, the speed of trucks ranges from 16 to 23 km/h when they are turning right [31], and the maximum speed is usually less than 32 km/h [17]. Considering the actual driving environment, the right-turn scenario simulation examined speeds of 15 km/h, 20 km/h, 25 km/h, and 30 km/h. The semitrailer truck model was placed at the original position and turned according to the defined path with four sets of speeds without any braking strategy. Consequently, the formation of and variation in the blind zone due to the inner wheel difference can be obtained during the right turn.

Moreover, as a semitrailer truck usually adopts an articulated connection, the driver dynamically changes the angle during the turning process. Specifically, the effect of the wheel track difference is significant, because the instantaneous steering centers of the tractor and trailer do not coincide, and the turning trajectory is not a regular circular arc. Therefore, different combinations of minimum turning radii r_1 and r_2 for the tractor and trailer were used in the simulation to examine the influence of the turning radius on the range of the inner wheel difference. In terms of the minimum turning radius of a semitrailer truck during a right turn, the minimum turning radius of the tractor is in the range of 8–12 m, and the trailer will produce a certain degree of lateral deflection during the turning process due to the hysteresis of the movement. Then, three sets of minimum turning radius combinations of the tractor (r_1) and trailer (r_2) were selected in the simulation test: (a) $r_1 = 8$ m and $r_2 = 10$ m, (b) $r_1 = 10$ m and $r_2 = 13$ m, and (c) $r_1 = 12$ m and $r_2 = 16$ m.

In the simulation, the semitrailer truck was placed at the starting position in the intersection, and the initial turning speed was set to 20 km/h. By adjusting the path point of the semitrailer truck during the right turn, the turning trajectory and the inner wheel difference blind zone were recorded with three groups of minimum turning radius combinations.

(2)   Simulation test for accident severity based on collision position.

The body length of a semitrailer truck is usually greater than 13 m. The collision positions of two-wheeled non-motorized vehicles and semitrailer trucks in accidents were found to be closely related to accident severity. To further investigate the influence on the accident risk when the object is in different relative positions to the semitrailer, in the PC-CRASH simulation of crashes, the moment when the two are about to collide was used as the starting point of the right-turn process analysis, while the position and motion state of the right turn process were recorded. Moreover, the two-wheeled vehicle and the rider were placed within the five collision zones to simulate the collision, and damage was recorded.

4. Results

4.1. Blind Zone Calculation Model for the Inner Wheel Difference

The calculation of the right-turn trajectory of the semitrailer truck is necessary to obtain the inner wheel difference blind zone. During the test, the coordinate points of the first and sixth axle wheel trajectories in the right-turn process were selected sequentially, as well as the calculated angles between the tractor and the trailer, which are collated in Table 2. The results are plotted in Figure 6, and the maximum width between the wheel trajectories of the first and sixth axles of the semitrailer is 4.4 m, which means the maximum width of the inner wheel difference blind zone during the right turn is 4.4 m.

To establish the calculation model for the blind zone from the inner wheel difference, the formation of the inner wheel difference for a rigid truck is shown in Figure 7, and

the equation for calculating the inner wheel difference ΔR_0 is expressed as Equation (1). The inner wheel difference test data of the semitrailer truck were calculated according to Equation (1).

$$\Delta R_0 = \sqrt{\left(\sqrt{r^2 - l^2} - k\right)^2 + l^2} - \sqrt{r^2 - l^2} + k \tag{1}$$

where r is the minimum turning radius of the left wheel of the first axle, which is also the distance OA$'$; l is the wheelbase between the first and last axle, and k is the tread.

Table 2. Blind zone data during the right turn of the semitrailer truck.

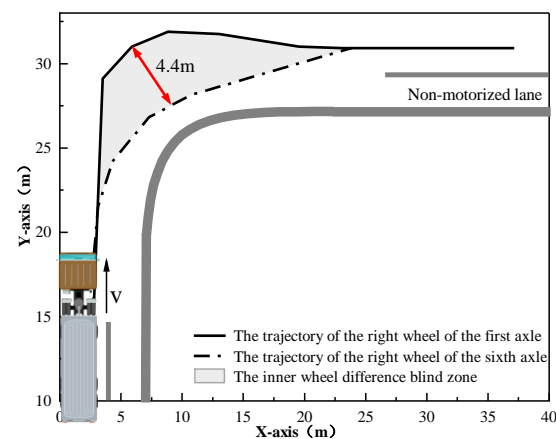| Right-Side Wheel Coordinates/m		Angle of Tractor and Trailer/($^\circ$)
First Axle	**Sixth Axle**	
(2.75, 15.24)	(2.75, 1.92)	0
(3.50, 29.10)	(2.75, 16.13)	21.12
(5.89, 31.00)	(2.77, 18.80)	30.63
(8.85, 31.90)	(3.03, 21.54)	47.68
(13.02, 31.75)	(4.31, 24.21)	63.5
(19.56, 31.00)	(7.28, 26.82)	28.8
(23.05, 30.93)	(10.70, 28.14)	20.28
(37.15, 30.93)	(23.83, 30.93)	0

Figure 6. The wheel tracks and inner wheel difference blind zone.
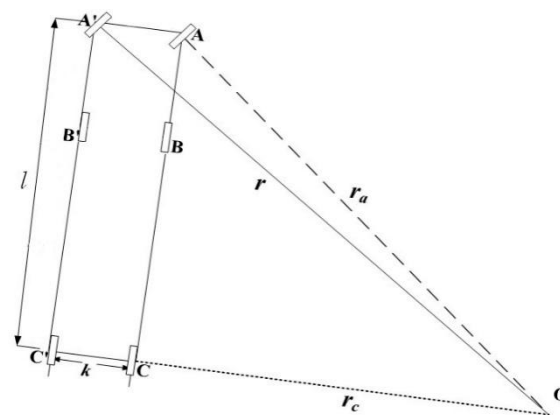

Figure 7. Inner wheel difference formation for rigid trucks.

Through calculation, the maximum width of the inner wheel difference blind zone was found to be 5.59 m, which is different from the test results. This is mainly caused by the trajectory difference between the semitrailer truck and the trajectory of a rigid truck. For the right turn of a rigid vehicle, the ratio of the inner wheel difference is in accordance

with the Ackermann principle [32], based on which the vehicle shape does not change during the turning process and does not produce a relative turning angle. Thus, its inner wheel difference ΔR_0 is mainly influenced by the turning radius, tread, and wheelbase. However, a semitrailer truck is an articulated truck connected to the tractor via a traction pin, and there is no steering device for the trailer body. As the truck turns right, the steering angle generated by the first axle is transferred to the second and third axles, and the tractor transmits the right-turn angle to the tires of each axle of the trailer through the traction pin. During the turning process, the angle between the tractor and trailer changes, which is not in accordance with the Ackermann principle [33].

To accurately calculate the wheel trajectory during the right turning of a semitrailer truck, Equation (1) was modified, as shown in Figure 8. BB″ was introduced as a virtual axle, while B″ and B indicate the left and right wheels, respectively. In addition, a virtual axle, assumed in the same position as the third axle of the tractor in the trailer part and parallel to the other axle of the trailer, was used as the steering axle, whose direction was the same as the direction of the force on the front edge of the trailer. The virtual axle can maintain the steering effect from the tractor on the trailer, while the two parts of the vehicle body are still independent. Therefore, the right-turn inner wheel difference ΔR was calculated as expressed in Equation (2). Based on the parameters in the field test of the semitrailer truck and Equation (2), the maximum inner wheel difference was calculated as 4.42 m, which is close to the maximum width of the inner wheel difference obtained from the test. Therefore, it is believed that the theoretical model could be used to obtain the maximum inner wheel difference for different types of semitrailer trucks.

$$\Delta R = R_a - R_b + R_{b'} - R_c$$
$$= \sqrt{\left(\sqrt{r_1^2 - l_1^2} - k_1\right)^2 + l_1^2} + \sqrt{\left(\sqrt{r_2^2 - l_2^2} - k_2\right)^2 + l_2^2} - \sqrt{r_1^2 - l_1^2} - \sqrt{r_2^2 - l_2^2} + k_1 + k_2 \tag{2}$$

where R_a is the turning radius of the right wheel of the first axle, i.e., the distance OA; R_b is the turning radius of the right wheel of the third axle, i.e., the distance OB; $R_{b'}$ is the distance of the turning radius O′B of the right wheel of the virtual axle; R_c is the distance of the turning radius O′C of the right wheel of the sixth axle; r_1 is the distance of the minimum turning radius OA′ of the left wheel of the first axle; r_2 is the distance of the minimum turning radius O′B″ of the left wheel of virtual axle; k_1 is the tread of the tractor; k_2 is the tread of the trailer; l_1 is the wheelbase of the 1–3 axle; and l_2 is the wheelbase of 3–6 axle.
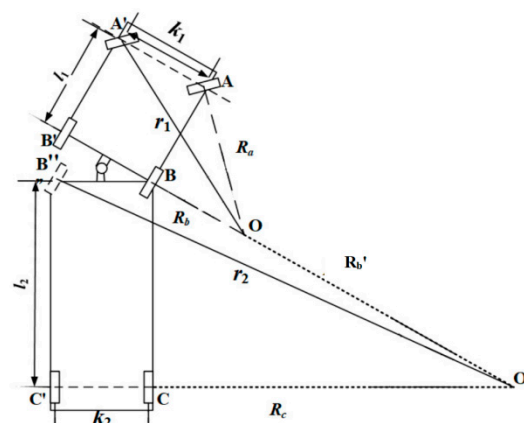

Figure 8. Right-turn trajectory formation of a semitrailer truck.

4.2. Effect of Turning Speed on the Blind Zone Due to the Inner Wheel Difference

Figure 9 shows the range of wheel tracks and blind zones from the inner wheel difference for semitrailer trucks at different turning speeds. To further analyze the relationship between speed and the blind zone, the maximum radial width of the blind zone and the minimum distance between the right wheel track of the sixth axle and the adjacent

shoulder during the right turn were measured using the PC-CRASH tape function, and the results are plotted in Figure 10. Notably, the turning speed affects the shape and maximum width of the blind zone resulting from the inner wheel difference. As the right-turn speed increases, the maximum width of the blind zone decreases significantly. Remarkably, the maximum width of the inner wheel difference blind zone reached 3.54 m at the minimum turning speed of 15 km/h for the semitrailer truck, while the widths were 3.28 m, 2.49 m, and 1.91 m at the right-turn speeds of 20 km/h, 25 km/h, and 30 km/h, respectively. A possible explanation is that large vehicles turning right at a higher initial speed with a large radius for a gentle turning operation will be safer compared to a sharp turn in the case of a small radius, which ensures the stability of the vehicle and avoids the dangerous situation brought about by a rapid increase in steering wheel angle, such as skidding or even rollover, although this is predicated on the safety of driving.
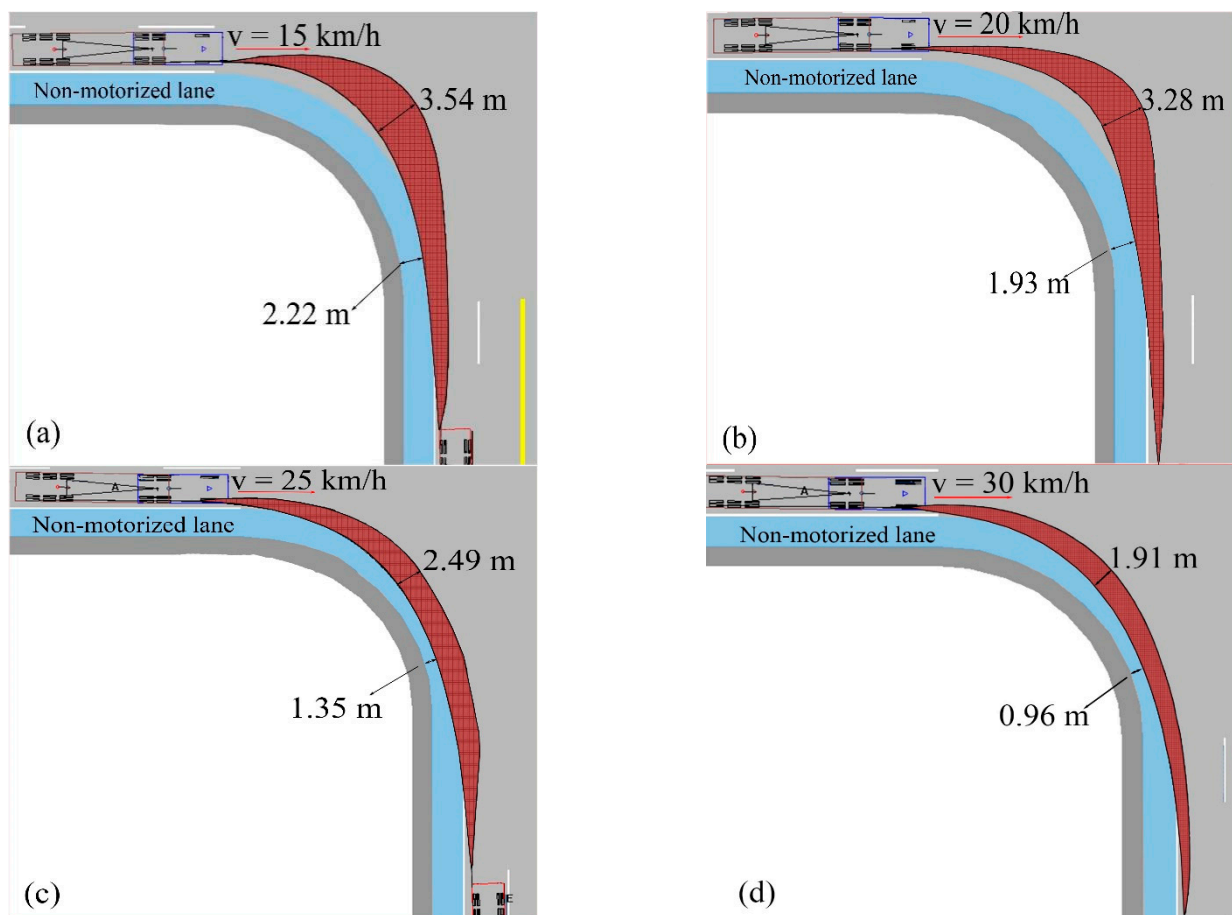

Figure 9. Blind zones from the inner wheel difference at different speeds: (**a**) v = 15 km/h, (**b**) v = 20 km/h, (**c**) v = 25 km/h, and (**d**) v = 30 km/h.

It is worth noting that a high turning speed leads to an overlap between the non-motorized lane and the blind zone from the inner wheel difference. The higher turning speed brings the truck's trajectory close to the non-motorized lane boundary, which increases the possibility of encroaching on the non-motorized space. According to the standards promulgated in China [34–36], the width of road space required for two-wheelers to go straight in a non-motorized lane is generally 0.45–0.81 m. The non-motorized lane space is likely to be occupied by a turning truck. For instance, when the right turn is performed at 30 km/h, the maximum width of the blind zone is only 1.91 m, and the minimum distance of the inner wheel difference blind zone boundary from the non-motorized lane boundary is only 0.96 m. Approximately 61.6% of non-motorized lanes will be occupied during the right-turn process.
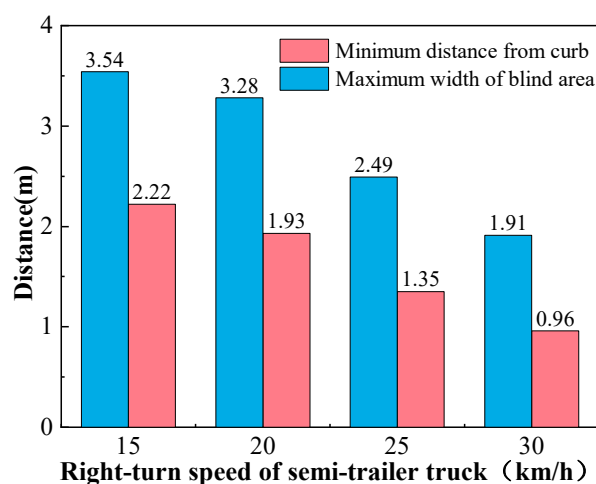
Figure 10. Influence of driving speed on the right turn of a semitrailer truck.

In addition, it is considered that a lower turning speed will facilitate the self-rescue of the two-wheeler rider to reduce the severity of the consequences. One of the common features of right-turn crashes at intersections is the driver's failure to detect an adjacent VRU before turning, and thus the driver fails to take any braking or evasive action until the crash occurs. For the driver, turning speed may not prevent the potential collision. However, from the two-wheel rider's perspective, low turning speed will give the VRU more time to be aware of dangerous situations and take self-rescue measures, such as abandoning the vehicle or swerving to prevent a collision. Therefore, considering the existing lane width standard, it is recommended that the right-turn speed of semitrailer trucks be less than 20 km/h.

4.3. Effect of the Turning Radius on the Blind Zone Due to the Inner Wheel Difference

Figure 11 shows the range of wheel tracks and inner wheel difference blind zones generated by the right-hand wheels of the first and sixth axles of the semitrailer truck at different turning radii. The turning radius affects the shape and maximum width of the blind zone from the inner wheel difference. As the turning radius decreased, the maximum width of the blind zone gradually increased, and its shape changed from a lanky moon shape to a fully curved moon shape. While the minimum turning radii $r_1 = 12$ m and $r_2 = 16$ m were reduced to $r_1 = 8$ m and $r_2 = 10$ m, respectively, the maximum width of the blind zone from the inner wheel difference increased from 2.55 m to 3.57 m. The size of the inner wheel difference blind zone was significantly affected by the turning radius, which also increased the collision risk with non-motorized vehicles. When turning with a small radius, the blind zone area from the rearview mirror of the semitrailer also increased sharply, which greatly increased the collision risk during the right turn. Additionally, the duration of the blind zone increased from 4.5 s to 5.6 s when the sum of r_1 and r_2 increased. Although the right turn of the semitrailer truck with a large turning radius increased the duration of the blind zone, the small width of the blind zone made the turn safer. Therefore, intersection design should control the radius parameter from the perspective of reducing right-turn accidents.

4.4. Impact of Collision Position on the Accident Risk Level

The accident statistics reported 185 two-wheeled riders and rear seat occupants, with 180 total casualties, including 89 fatalities, which indicates the severity of such crashes. Additionally, the statistical analysis indicated that the collision position is highly correlated with both the severity of an accident and fatality rates. The two front zones of a semitrailer truck, positions 1 and 2, are the zones with the highest frequency of collisions and the highest accident fatality rate, as shown in Figure 12. Among them, 61 and 45 accidents occurred in positions 1 and 2, respectively, accounting for 40.7% and 30% of the total

accidents, respectively. Specifically, 42 and 32 deaths were attributed to collisions at positions 1 and 2, respectively. However, although the number of fatalities in accidents at position 3 was lower, 12, it is still high. In contrast, the statistical parameters of positions 4 and 5 were significantly lower than those at other positions, but the danger of accidents cannot be ignored. It is worth noting that fatal accidents, which are mainly caused by riders in a blind zone experiencing secondary crushing injuries, rarely occur at position 5. Thus, this position had the lowest risk of accidents. In summary, the collision position is highly correlated with the frequency and severity of accidents. VRUs are exposed to great risk in right-turn collisions with large vehicles such as semitrailers. There is a close relationship between the collision position and accident hazard [11,37,38].
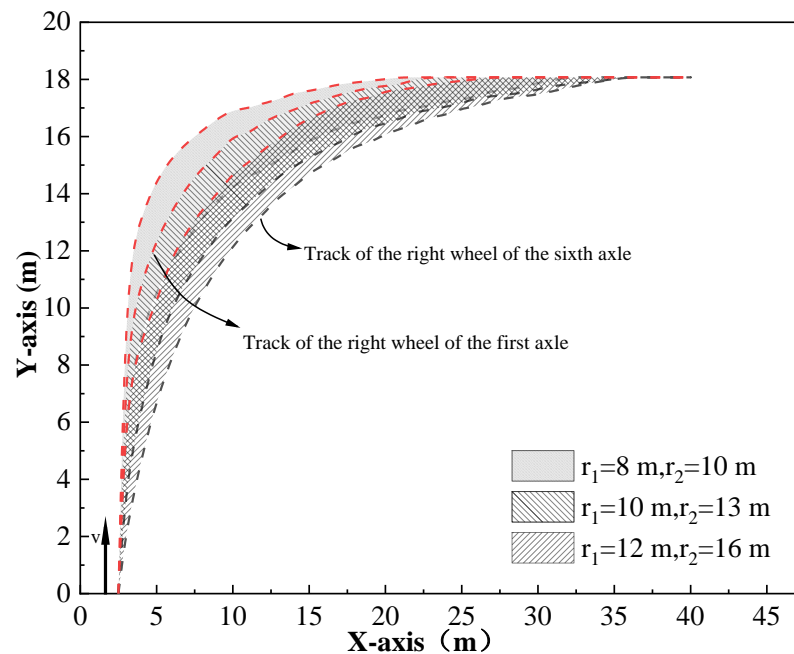
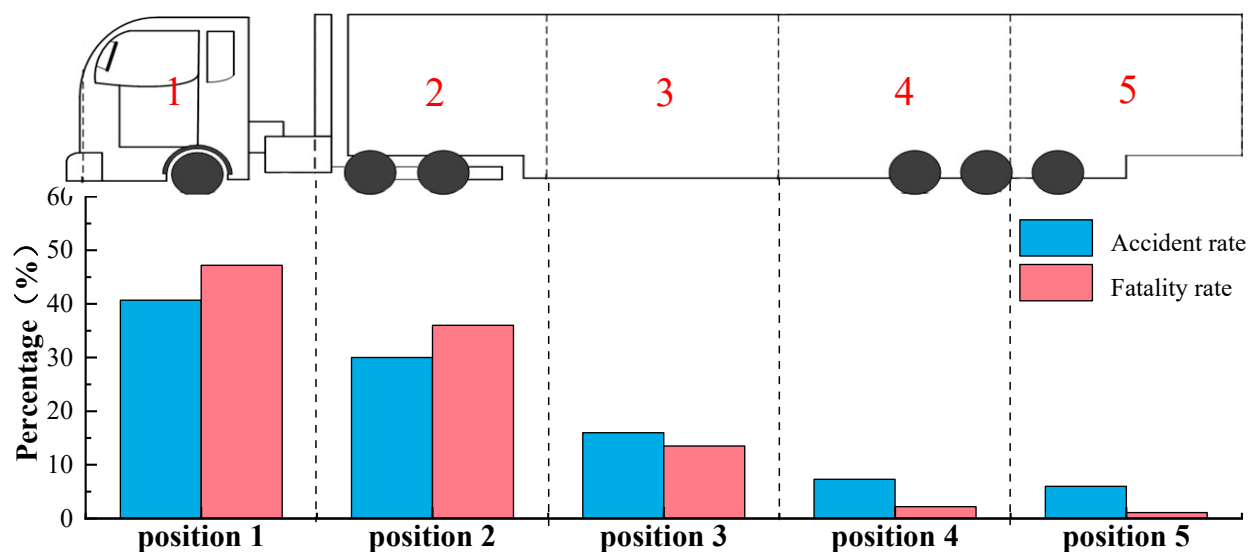**Figure 11.** Comparison of the right-turn blind zone of a semitrailer truck with different turning radii.
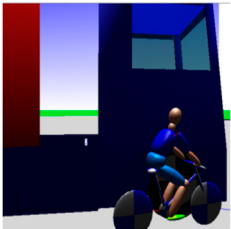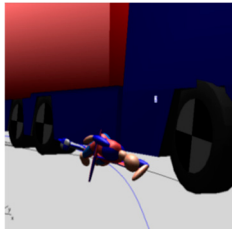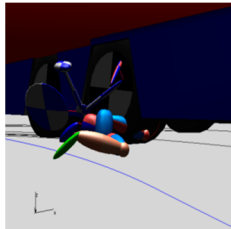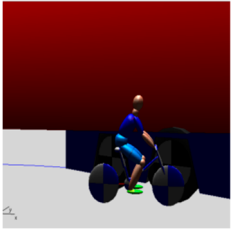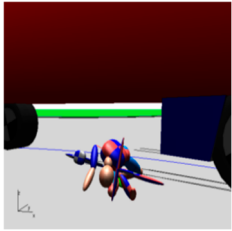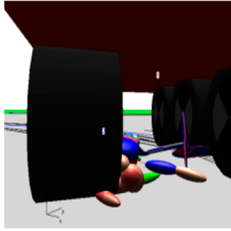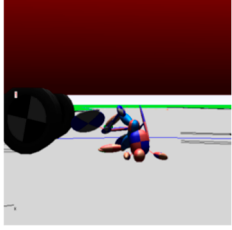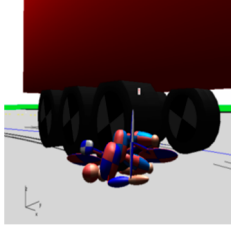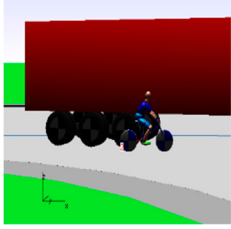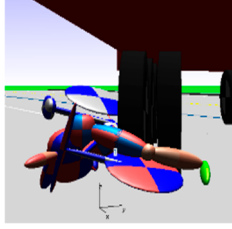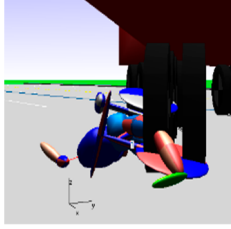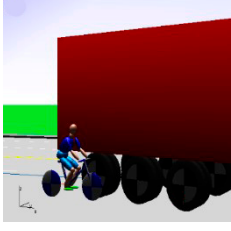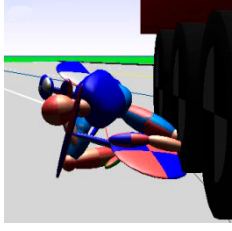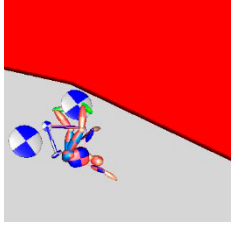
Figure 12. Proportion and accident severity in each division zone of a semitrailer truck.

The accident information was collected in the PC-CRASH simulation test with five crash positions, which is shown in Table 3. Notably, the simulation results again demonstrate that the collision position was significantly correlated with the crash severity. Forward position is more likely to cause a greater inner wheel difference blind zone and results in

rider risk of serious secondary injury caused by rider crush with the tires behind. In order to quantitatively assess the risk level of the collision, we chose the parameters of head acceleration and head injury criterion (HIC) as indicators of the degree of injury to the rider. It is worth noting that the standard HIC36 ($t_2 - t_1 \leq 36$ ms) threshold for head tolerance is 1000 [39], which when exceeded indicates that the object will be seriously injured or killed in the crash.

Table 3. Collision simulation of objects located at different positions along a semitrailer truck.

Collision Position	First Point of Contact	Landing Place	Secondary Injury	Injuries to Cyclist
1				The head was crushed by the right wheel of the second and third axles of the semitrailer
2				The middle of the body and upper limbs were crushed by the right wheel of the fourth axle of the semitrailer
3				The middle of the body and lower limbs were crushed by the right wheel of the fourth axle of the semitrailer
4				Lower limbs were crushed by the right wheel of the fourth axle of the semitrailer
5				Not crushed

The variation pattern of head acceleration with time for a two-wheeled rider in five collision scenarios was drawn in Figure 13. It can be found that there is a clear correspondence between the number of impacts on pedestrians and the number of peak head acceleration occurrences. Therefore, the entire collision process can be roughly divided into three stages: in the first stage, the two-wheeled vehicle collides with the semitrailer truck, and the first peak of the head acceleration curve of the rider appears. In the second stage, with the

second peak of the head acceleration curve, the rider falls to the ground. The third peak occurs in the third stage, when the rider falls to the ground and is within the blind zone from the inner wheel difference of the semitrailer truck, which can cause the rear wheels to crush the rider. The three-stage division is consistent with the findings of Wei et al. [15]. The number of times a rider's head acceleration peaks indicates the number of times the head is exposed to a hazard or collision. More time in the head acceleration peaks means higher risk of a crash.
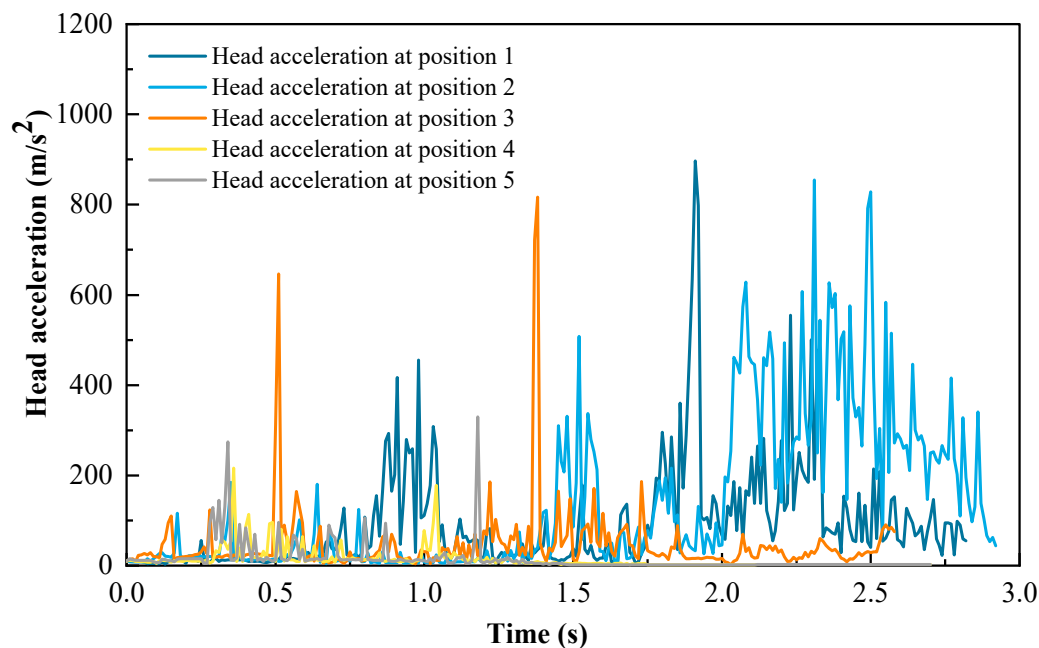
Figure 13. Head acceleration at different collision positions.

The third stage, i.e., the crushing process, is the key to the severity of the collision. Figure 13 shows that the maximum values of head acceleration during the collision occur in the third stage. When the cyclist collided with the semitrailer in position 1, the maximum head acceleration of the cyclist reached 897.1 m/s^2, and the maximum value of HIC appeared in the time range of 1.89–1.93 s, which was 1444.1. As the collision part was the head, the rider suffered fatal injury, and the risk of the crash was the highest. In the crash at position 2, the peak acceleration of the cyclist's head in the third stage was 628.19 m/s^2, and the maximum HIC was 1250.9. Although it is lower than that of position 1, it still exceeds the head tolerance limit, and the cyclist is likely to be fatally threatened. In the collision at position 3, the cyclist was crushed by the wheel during the period of 1.36–1.39 s. During this time, the peak head acceleration was 721.4 m/s^2, and the HIC was 626.5, which was lower than the tolerance limit of the head, but the damage was still serious. The study concluded that position 3 is the threshold position for fatal or not, and the collision with a two-wheeler in the front 3/5 L position along the vehicle has a very high fatality rate and risk. Compared with the above three positions, when the collision parts are located in position 4 and position 5, the danger of the crash is significantly reduced. In these two working conditions, the maximum value of the rider's head acceleration is 215.7 m/s^2 and 274.1 m/s^2, respectively, and the HIC is below 100, which is much smaller than the head tolerance limit. In conclusion, the front three collision positions along the semitrailer truck result in a high probability of secondary crushing injury and must be considered in safety management.

5. Discussion

5.1. Combined Effect of a Double-Blind Zone

There is high risk of collisions between large vehicles turning right and two-wheelers. Usually, people concerned with the blind zone for this type of crash focus especially

the blind zone due to the inner wheel difference, which may lead to secondary injuries. However, during the right turn of a large vehicle, there is also a blind zone in the rearview mirror, in addition to the blind zone from the inner wheel difference. Notably, the two blind zones do not exist independently of each other. The driver can only obtain restricted information around the vehicle when there is a large right-turn angle between the tractor and trailer and the view field of the right rearview mirror is dynamically reduced. We define the area where the view of right rearview mirror is reduced as the "failure area of the right rearview mirror". The failure area is within the blind zone of the inner wheel difference. This results in the combined effect of the blind zone of the rearview mirror and the blind zone of the inner wheel difference, which form a "double-blind zone" that is a factor in drivers failing to detect two-wheeled vehicles. To further examine the mechanism of the double-blind zone, the rearview mirror blind zone, the wheel trajectories of the first and sixth axles on the right side of the semitrailer, and the right rearview mirror view boundary coordinates in the same coordinate system were examined to determinethe dynamic change process of the right-turn blind zone. The intersection relationship of the double-blind zone is shown in Figure 14.
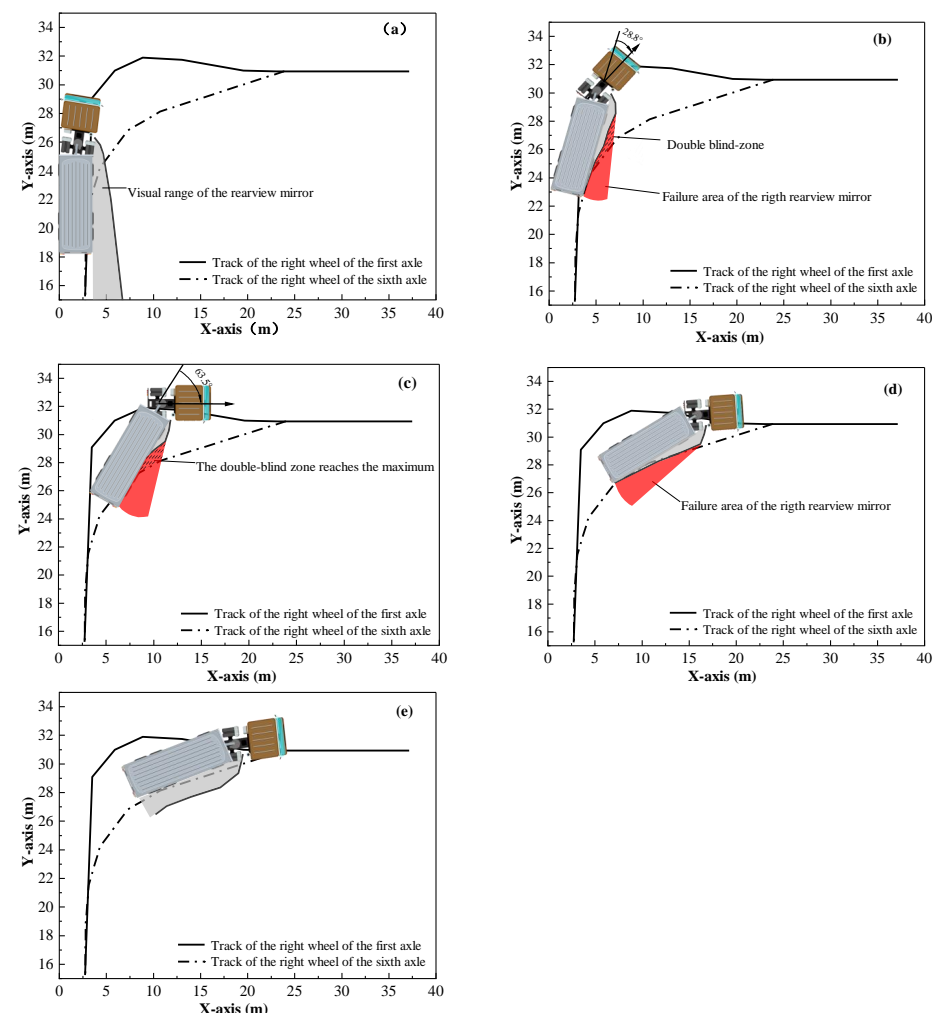
Figure 14. Process of a right turn in a double-blind zone: (**a**) at the beginning of the right turn, the right rearview mirror has the largest view; (**b**) the right rearview mirror can observe the entire body; (**c**) the scale of the double-blind zone reaches a maximum; (**d**) the scale of the double-blind zone range gradually dissipates; and (**e**) the right rearview mirror vision returns to normal.

The results of the double-blind zone analysis reveal that the interaction between the blind zone caused by the inner wheel difference and rearview mirror increases the accident

risk and fatality rate. During the right turn of the semitrailer truck, the blind zone caused by the inner wheel difference and rearview mirror varies with the turning angle of the tractor and trailer. Increasing the turning angle increases the scale of the two blind zones. At the beginning of the right turn of the vehicle, the angle between the tractor and trailer ranges from 0° to 20.5°, and the blind zone from the inner wheel difference can be observed in the rearview mirror, as shown in Figure 14a. Thus, the driver of a semitrailer truck can completely observe the two-wheeled rider and avoid collision accidents. When the angle between the tractor and trailer is equal to or greater than 20.5°, the blind zone from the inner wheel difference begins to overlap with the blind zone from the rearview mirror. Thus, the driver is unable to observe the two-wheeled rider in the overlapping zone from the right rearview mirror, and as the truck continues to move forward, the rider will suffer the risk of being run over, which is a dangerous situation.

When the angle reaches 28.8°, as shown in Figure 14b, the driver's vison from the right rearview mirror can only reach the trailer's rear position. As the turning angle continues to increase, the driver can no longer see the entire vehicle body. When the angle reaches the maximum value of 63.5° in the turning process, the driver's vison from the rearview mirror in terms of vehicle length is the shortest, that is, 4 m. As Figure 14c shows, the width of the inner wheel difference blind zone reaches a maximum of 4.4 m, and the blind zone of the rearview mirror is also in the maximum state, which indicates that the right rearview mirror fails the most seriously at this time. From the start of the right turn to this position, the scale of the blind zone caused by the inner wheel difference and the failure area of the right rearview mirror gradually increases with the turn angle. Additionally, the overlapping zone of the double-blind zone increases until the overlapping shape changes from a narrow shape to a diamond, which is defined as the "right turn double-blind zone mechanism" in this study. The interaction mechanism of the double-blind zone makes the driver unable to observe the two-wheeled vehicles and pedestrians around the vehicle, which is the main reason for collisions and the crushing of two-wheeled riders.

Subsequently, the semitrailer truck turns right and enters the second stage, as shown in Figure 14d,e. The angle between the tractor and trailer gradually reduces, while the blind zone of the rearview mirror gradually separates from the blind zone caused by the inner wheel difference and eventually reverts to normal. The inner wheel difference blind zone continues to exist until the right turn is completed, and the tractor and trailer travel in a straight line. Therefore, the existence of a double-blind zone for right turning leads to dangerous driving behavior, as drivers become unable to observe surrounding objects.

5.2. Right-Turn Accident Prevention and Control

Large vehicles are commonly driven on urban roads, especially with the rapid development of the logistics industry. For instance, large semitrailer trucks are mostly driven at night, which also increases the blind zone areas during right turns and the probability of accidents. Large articulated vehicles have the largest blind zones. There are also some other nonarticulated large vehicles, such as concrete trucks, buses, and garbage trucks, which have blind zones when turning right. However, the blind zones of these vehicles, generated via different mechanisms, result in accidents with low risk, which should also be considered. Therefore, various management strategies should be utilized to address such types of traffic accidents, their prevention, and control measures, which may begin with many aspects such as people, vehicles, and roads.

First, drivers must be made aware of the existence of blind zones and the serious risk of accidents they pose through publicity and training, such as the introduction of compulsory tests on blind zone accidents and blind zone formation as part of the testing for driving permits. Drivers should be reminded to be aware of the surrounding traffic participants when turning right [16]. In addition, the summaries of such accidents show that the misunderstandings of non-motor vehicle riders about the vision ability of truck drivers are also an important cause of accidents [19]. Non-motorists always believe that vehicle drivers can observe them and are able to yield during a right turn. This misconception also

causes the non-motorists to maintain a straight line or even make a dangerous overtaking move. Therefore, non-motorists should be trained about the risks of right-turn blind zones and actively avoid large trucks that are making a right turn.

Moreover, the structural characteristics of vehicles that are directly related to blind zones should be improved to eliminate blind zones. Generally, the visibility of drivers can be improved by increasing the number of mirrors on vehicles to a maximum of six [13]. However, collisions still occur, because it is difficult for the driver to scan multiple mirrors during turns and obtain sufficient information about the surroundings of the vehicle body. The application of a blind zone warning system can effectively solve this problem. Relying on ultrasonics, radar, infrared induction, and other technical means, drivers' blind zone elimination devices and cyclist-identification devices will become the necessary equipment for heavy freight vehicles [40]. Industry management departments should promote such equipment and mandatory inspection of vehicles in standards or laws. For example, in China, to reduce the number of right-turn collisions due to blind zones, the government has developed specifications such as SAMR 2020a, 2020b [41,42] for vehicles to install right-turn behavior detection and warning devices. These efforts have played a positive role in reducing right-turn accidents. For the inner wheel difference blind zone that exists during right turns, a laser-projection warning device installed in the vehicle can determine the range of the inner wheel difference blind zone according to the real-time turning radius. Simultaneously, the device can emit a laser to the corresponding zone to form a colored blind risk warning area on the road surface to remind traffic participants to maintain a safe distance from a right-turning vehicle [4]. In this study, the collision position was found to have a direct relationship with the accident rate and severity. Installing an infrared sensing device within the vehicle at positions 1 to 3 to identify VRUs could effectively reduce the occurrence of right-turn accidents. With the development of digital technology, multifunctional, integrated-imaging, and human-identification devices no longer pose technical problems. The development of convenient and practical blind-zone elimination devices should be further studied.

Finally, roadside facilities can effectively improve driving environments. Although the blind zone caused by the inner wheel difference cannot be completely eliminated due to vehicle characteristics, VRUs can be kept away from right-turning trucks. For instance, a right-turn warning zone can be marked in color on the surface at intersections to alert VRUs in potential blind zones. In the design of the intersection, the right-turn lane is set up as a separate dedicated lane type, so that it turns right in advance to achieve the maximum separation from non-motorized vehicles. In addition, measures such as setting right-turn-only signals and installing barriers to separate motor vehicles from non-motor vehicles can improve intersection safety [12].

6. Conclusions

Blind zones are still a major safety issue for drivers and VRUs during the right turns of large vehicles in intersections. Although existing studies have addressed the factors influencing the scale of the blind zone and accident risk levels in right-turn collisions, the formation of blind zones and accident severity in right-turn collisions between articulated semitrailer trucks and two-wheeled vehicles is still unclear. Thus, factors such as the turning speed, turning radius, and collision position were investigated in the study, and the mechanism of the double-blind zone caused by the rearview mirror and inner wheel difference during the turning process was also studied.

To measure the scale of the inner wheel difference, a computational model of the right-turn blind zone for a semitrailer truck was proposed and applied. The proposed model follows the kinematic characteristics of a turning articulated semitrailer truck. By introducing a virtual axle, the estimation of the blind zone range was more accurate. The estimated blind zone can be used as a reference for road design.

The turning speed and turning radius of a semitrailer truck were found to affect the parameters of the blind zone due to the inner wheel difference, such as the shape,

area, maximum width, and occupation of the non-motorized lane. The results indicate that the blind zone caused by the inner wheel difference decreases with increasing right-turn speed of a semitrailer truck. However, a high speed is still more likely to result in the occupation of more space in the non-motorized lane by the semitrailer truck and a low reaction time for the driver and the VRU. However, the size of the turning radius is restricted by the geometric design of the intersection. Compared to a small turning radius, a large turning radius reduces the maximum width of the inner wheel difference blind zone, which increases the blind zone duration and potential for conflict between vehicles. Therefore, it is necessary to comprehensively consider the geometric design and actual operation of an intersection to restrict the thresholds of these two factors.

Notably, the position of the collision was found to significantly affect the severity of the accident. Secondary crushes were the main cause of fatal injuries in an accident. The closer the position of the first collision point is to the first axle of the vehicle, the higher the accident risk and injury rating. Thus, measures such as vehicle blindness remediation should be developed differently for various positions.

Moreover, the interaction between the blind zones resulting from the rearview mirror and the inner wheel difference further reduces the driver's effective field of vision. During the right turn of a semitrailer, these two blind zone areas increase and overlap simultaneously with an increasing turning angle. Thus, the long duration of the double-blind zone causes the driver to ignore riders, which may lead to a secondary crush within the blind zone range due to the inner wheel difference. The right rearview mirror field of view increases with the semitrailer turning angle and shows a dynamic reduction in the visible body length range, which is often overlooked.

It is worth emphasizing that our accident data are derived from related reports on the internet, so a significant number of minor collisions or accidents may have been missed. In addition, although the method of obtaining right-turn crash patterns by PC-CRASH is effective, the simulation process is limited to a single factor, without considering the chance and complexity of real crashes. Moreover, the differences in road conditions, vehicles, and manikins in different countries and regions should also be considered. Through crash simulations with PC-CRASH, influencing factors, such as rider speed, fall position, and reproduction of the accident with joint human–vehicle participation, will be further studied in future research. The results of this study also provide new insights into the causes of right-turn collisions and support traffic safety management at intersections.

Appendix A

Table A1. Accident Statistics.

Number	Time	Location	Casualties	Object Type	Collision Position
1	2018.10.08	Meizhou	One injured	Electric bicycle	2
2	2018.10.26	Shenzhen	One death	Bicycle	1
3	2018.10.24	Yangzhou	One death	Electric bicycle	1
4	2018.11.11	Hangzhou	One death	Electric bicycle	2
5	2018.11.16	Qinzhou	One injured	Electric bicycle	3

Table A1. *Cont.*

Number	Time	Location	Casualties	Object Type	Collision Position
6	2018.11.16	Qinzhou	One injured	Electric bicycle	5
7	2018.11.17	Taizhou	One injured	Electric bicycle	3
8	2018.11.20	Hangzhou	One injured	Electric bicycle	4
9	2018.12.12	Weifang	One death	Electric bicycle	2
10	2018.12.17	Linyi	One death	Electric bicycle	2
11	2018.12.27	Jinhua	One injured	Electric bicycle	5
12	2018.12.28	Nanning	One death	Electric bicycle	3
13	2019.01.05	Weifang	One injured	Electric bicycle	4
14	2019.01.06	Hangzhou	One injured	Electric bicycle	1
15	2019.01.07	Changsha	One death	Pedestrian	2
16	2019.01.10	Yangzhou	Two injured	Electric bicycle	2
17	2019.01.12	Shanghai	One death	Bicycle	2
18	2019.01.19	Longxi	One injured	Pedestrian	4
19	2019.02.08	Ma'anshan	One death	Electric bicycle	3
20	2019.02.09	Wenzhou	One death	Bicycle	1
21	2019.02.27	Changshu	One death	Electric bicycle	3
22	2019.03.01	Tengzhou	One death	Electric bicycle	1
23	2019.03.17	Jinan	One death	Bicycle	2
24	2019.03.17	Xiaoshan	One injured	Bicycle	1
25	2019.03.18	Chongqing	One injured	Motorcycle	1
26	2019.03.18	Shijiazhuang	One injured, one death	Electric bicycle	2
27	2019.03.22	Yulin	Three deaths	Electric bicycle	2
28	2019.03.28	Zaozhuang	One death	Electric bicycle	2
29	2019.04.02	Pucheng	Two injured	Motorcycle	2
30	2019.04.02	Shanghai	One death	Electric bicycle	3
31	2019.04.02	Baoshan	One death	Bicycle	2
32	2019.04.10	Fuyang	Two injured	Electric bicycle	5
33	2019.04.14	Zhengzhou	One injured	Electric bicycle	1
34	2019.04.16	Qinzhou	One injured	Motorcycle	3
35	2019.04.16	Nanning	Two injured, two deaths	Electric bicycle	1
36	2019.04.19	Yulin	One injured, one death	Motorcycle	3
37	2019.04.19	Harbin	One death	Pedestrian	3
38	2019.04.19	Yulin	One injured, one death	Motorcycle	2
39	2019.04.20	Beijing	Two deaths	Electric bicycle, bicycle	1
40	2019.04.23	Taiyuan	Two deaths	Electric bicycle	2
41	2019.04.24	Cenxi	No casualties	Electric bicycle	1
42	2019.04.29	Yueqing	One injured	Bicycle	4
43	2019.04.30	Haikou	One death	Electric bicycle	2
44	2019.05.03	Cangnan	One injured	Electric bicycle	1
45	2019.05.03	Lishui	One injured	Electric bicycle	1
46	2019.05.03	Yangzhou	Two injured, one death	Electric bicycle	1
47	2019.05.06	Jiaozuo	One injured	Electric bicycle	1
48	2019.05.08	Changxing	One death	Electric bicycle	2
49	2019.05.08	Yantai	One injured	Electric bicycle	2
50	2019.05.08	Yantai	Two deaths	Electric bicycle	1
51	2019.05.09	Wendeng	One death	Electric bicycle	2
52	2019.05.09	Quzhou	One injured	Electric bicycle	2
53	2019.05.10	Nanjing	One injured	Electric bicycle	4
54	2019.05.14	Xuancheng	One injured	Electric bicycle	2
55	2019.05.14	Ningbo	One injured	Electric bicycle	2
56	2019.05.14	Wenzhou	One injured	Electric bicycle	3
57	2019.05.16	Liuzhou	Two injured	Electric bicycle	2
58	2019.05.16	Guangxi	Two injured	Electric bicycle	1
59	2019.05.17	Wenzhou	One injured	Pedestrian	3
60	2019.05.20	Cangnan	One injured	Electric bicycle	2
61	2019.05.20	Xuancheng	One injured	Electric bicycle	1
62	2019.05.22	Baishan	One injured	Electric bicycle	2
63	2019.05.22	Wenzhou	One injured	Pedestrian	4
64	2019.05.22	Huaian	One injured	Electric bicycle	5
65	2019.05.23	Linyuan	One death	Motorcycle	3

Table A1. *Cont.*

Number	Time	Location	Casualties	Object Type	Collision Position
66	2019.05.24	Zhenjiang	One injured	Electric bicycle	5
67	2019.05.27	Xi'an	One death	Electric bicycle	4
68	2019.05.30	Nanchang	One death	Bicycle	1
69	2019.05.31	Zhenjiang	One injured	Electric bicycle	5
70	2019.06.04	Shunde	One injured	Bicycle	4
71	2019.06.06	Hangzhou	One death	Electric bicycle	3
72	2019.06.07	Laibin	Two deaths	Electric bicycle	1
73	2019.06.11	Liaoccheng	One death	Electric bicycle	2
74	2019.06.12	Shunde	One death	Electric bicycle	2
75	2019.06.13	Zhumadian	One injured	Electric bicycle	2
76	2019.06.14	Shunde	One death	Pedestrian	3
77	2019.06.22	Yangzhou	One injured, one death	Electric bicycle	1
78	2019.06.23	Xiaoshan	One injured, one death	Electric bicycle	1
79	2019.06.24	Xuancheng	One injured	Electric bicycle	3
80	2019.07.11	Ningbo	One injured	Electric bicycle	2
81	2019.07.24	Taiwan	One injured	Motorcycle	1
82	2019.07.24	Guangzhou	One injured	Electric bicycle	1
83	2019.08.05	Ma'anshan	One death	Bicycle	2
84	2019.08.12	Changzhou	One death	Electric bicycle	1
85	2019.08.15	Zibo	One injured	Electric bicycle	3
86	2019.08.16	Hangzhou	One injured, one death	Electric bicycle	3
87	2019.08.16	Dongwan	Three deaths	Electric bicycle	1
88	2019.08.20	Liuzhou	One injured	Electric bicycle	1
89	2019.08.20	Zhangjiagang	One injured	Electric bicycle	1
90	2019.08.24	Chengdu	One injured	Electric bicycle	5
91	2019.08.27	Fuzhou	One death	Electric bicycle	1
92	2019.08.28	Quanzhou	One death	Bicycle	2
93	2019.08.30	Jiaxing	One death	Bicycle	1
94	2019.08.31	Huanbei	One injured	Electric bicycle	1
95	2019.09.02	Chuzhou	One death	Electric bicycle	2
96	2019.09.03	Lishui	No casualties	Electric bicycle	3
97	2019.10.19	Yibin	One injured, two deaths	Electric bicycle	1
98	2019.11.03	Weifang	One death	Electric bicycle	1
99	2019.11.11	Hangzhou	One death	Electric bicycle	1
100	2019.11.16	Qinzhou	No casualties	Electric bicycle	3
101	2019.11.17	Taizhou	One injured	Electric bicycle	2
102	2019.11.20	Foshan	One injured	Electric bicycle	3
103	2019.11.26	Beihai	One injured	Bicycle	1
104	2019.12.7	Dongwan	Two injured, one death	Motorcycle	4
105	2019.12.8	Zhejiang	One injured	Electric bicycle	1
106	2019.12.17	Ningbo	One injured	Electric bicycle	2
107	2019.12.20	Guangdong	One death	Bicycle	1
108	2020.01.13	Sichuan	One injured, one death	Electric bicycle	5
109	2020.03.17	Shandong	One death	Electric bicycle	2
110	2020.04.8	Changsha	One death	Electric bicycle	1
111	2020.05.8	Yibin	Two deaths	Electric bicycle	1
112	2020.05.13	Suzhou	No casualties	Electric bicycle	1
113	2020.05.14	Beihai	One death	Electric bicycle	2
114	2020.05.15	Tangshan	One injured	Electric bicycle	5
115	2020.05.16	Zhengzhou	One injured	Pedestrian	3
116	2020.06.01	Qinzhou	One injured, one death	Motorcycle	2
117	2020.06.13	Shanghai	One death	Electric bicycle	1
118	2020.06.25	Xinzhou	Two injured	Electric bicycle	1
119	2020.07.01	Rizhao	One death	Electric bicycle	1
120	2020.07.02	Yancheng	One injured, one death	Electric bicycle	1
121	2020.07.09	Liuzhou	One death	Electric bicycle	1
122	2020.07.11	Dezhou	One injured, one death	Electric bicycle	2
123	2020.07.16	Handan	One death	Electric bicycle	2
124	2020.07.16	Zhejiang	One death	Bicycle	1
125	2020.07.23	Chenzhou	One injured	Motorcycle	1

Table A1. *Cont.*

Number	Time	Location	Casualties	Object Type	Collision Position
126	2020.07.24	Tangshan	One injured	Electric bicycle	4
127	2020.07.30	Hangzhou	One injured	Electric bicycle	1
128	2020.08.07	Tai'an	One death	Electric bicycle	2
129	2020.08.21	Nanyang	One death	Motorcycle	1
130	2020.08.24	Liuzhou	One death	Motorcycle	1
131	2020.08.24	Meishan	One death	Motorcycle	2
132	2020.08.31	Changsha	One injured, one death	Electric bicycle	1
133	2020.09.07	Shanghai	One death	Bicycle	1
134	2020.09.11	Qingdao	One injured	Electric bicycle	2
135	2020.09.21	Liuzhou	One death	Electric bicycle	1
136	2020.09.25	Hangzhou	One injured	Electric bicycle	1
137	2020.10.03	Hangzhou	One injured	Electric bicycle	2
138	2020.10.09	Linfen	One death	Electric bicycle	2
139	2020.10.14	Shanghai	One death	Electric bicycle	3
140	2020.10.30	Zhenjiang	One injured	Electric bicycle	1
141	2020.11.08	Hangzhou	One injured	Electric bicycle	1
142	2020.11.11	Jining	One injured	Electric bicycle	1
143	2020.11.11	Yulin	One death	Electric bicycle	1
144	2020.11.16	Hangzhou	One injured	Electric bicycle	1
145	2020.11.17	Jilin	One death	Electric bicycle	2
146	2020.11.26	Liuzhou	One death	Motorcycle	1
147	2020.12.19	Wenzhou	One death	Bicycle	1
148	2020.12.21	Sanmenxia	Two injured	Electric bicycle	3
149	2020.12.21	Ningbo	No casualties	Electric bicycle	4
150	2020.12.27	Liuzhou	One death	Motorcycle	3

References

1. Pokorny, P.; Drescher, J.; Pitera, K.; Jonsson, T. Accidents between freight vehicles and bicycles, with a focus on urban areas. *Transp. Res. Procedia* **2017**, *25*, 999–1007. [CrossRef]
2. Sitao, H.; Qiaojun, X.; Huihui, X.; Gang, X. Safety impact analysis of large vehicles' right-turn on pedestrians and non-motorized vehicle at signalized intersection. In Proceedings of the World Automation Congress, Puerto Vallarta, Mexico, 24–28 June 2012; pp. 1–4.
3. Jia, Y.; Cebon, D. Field Testing of a Cyclist Collision Avoidance System for Heavy Goods Vehicles. *IEEE Trans. Veh. Technol.* **2016**, *65*, 4359–4367. [CrossRef]
4. Zhang, Q.; Wei, Y.; Wang, K.; Liu, H.; Xu, Y.; Chen, Y. Design of Arduino-Based In-vehicle Warning Device for Inner Wheel Difference. In Proceedings of the 2019 IEEE 2nd International Conference on Electronics Technology (ICET), Chengdu, China, 10–13 May 2019; pp. 301–304.
5. Talbot, R.; Reed, S.; Christie, N.; Barnes, J.; Thomas, P. Fatal and serious collisions involving pedal cyclists and trucks in London between 2007 and 2011. *Traffic Inj. Prev.* **2017**, *18*, 657–665. [CrossRef]
6. Malczyk, A.; Bende, J. Heavy Truck Crashes Involving Pedestrians in Comparison to Bicyclists. In Proceedings of the 26th International Technical Conference on the Enhanced Safety of Vehicles (ESV): Technology: Enabling a Safer Tomorrow National Highway Traffic Safety Administration (No. 19-0080), Eindhoven, The Netherlands, 10–13 June 2019.
7. Twisk, D.; Vlakveld, W.; Mesken, J.; Shope, J.T.; Kok, G. Inexperience and risky decisions of young adolescents, as pedestrians and cyclists, in interactions with lorries, and the effects of competency versus awareness education. *Accid. Anal. Prev.* **2013**, *55*, 219–225. [CrossRef]
8. Zhang, Z. Collision simulation of trucks and pedestrians based on Pc-Crash in the blind area of truck driving. In Proceedings of the SPIE 12058, Fifth International Conference on Traffic Engineering and Transportation System (ICTETS 2021), Chongqing, China, 24–26 September 2021. [CrossRef]
9. Moore, D.N.; Schneider, W.H., IV; Savolainen, P.T.; Farzaneh, M. Mixed logit analysis of bicyclist injury severity re-sulting from motor vehicle crashes at intersection and non-intersection locations. *Accid. Anal. Prev.* **2011**, *43*, 621–630.
10. Jannat, M.; Tapiro, H.; Monsere, C.; Hurwitz, D.S. Right-Hook Crash Scenario: Effects of Environmental Factors on Driver's Visual Attention and Crash Risk. *J. Transp. Eng. Part A Syst.* **2020**, *146*, 04020026. [CrossRef]
11. Niewoehner, W.; Berg, F.A. Endangerment of pedestrians and bicyclists at intersections by right turning trucks. In Proceedings of the 19th International Technical Conference on the Enhanced Safety of Vehicles (ESV), Washington DC, USA, 6–9 June 2005.
12. Bao, Y.; Wang, P.; Li, Y. Research on the optimization design of intersections for safe operation of large trucks. *J. Inf. Hiding Priv. Prot.* **2020**, *2*, 143–154. [CrossRef]

13. Summerskill, S.; Marshall, R.; Cook, S.; Lenard, J.; Richardson, J. The use of volumetric projections in Digital Human Modelling software for the identification of Large Goods Vehicle blind spots. *Appl. Ergon.* **2016**, *53*, 267–280. [CrossRef] [PubMed]

14. Tsai, C.-Y.; Sung, C.-K. Algebraic General Trajectory Formula for Semitrailer Truck Vehicles. *IEEE Trans. Autom. Sci. Eng.* **2020**, *18*, 2156–2165. [CrossRef]

15. Wei, L.; Tan, Y.; Liu, H.; Pu, Y. Electric cyclist injury of the collision between right turn of truck and electric bicycle. *Comput. Methods Biomech. Biomed. Eng.* **2021**, *24*, 1463–1472. [CrossRef]

16. Pokorny, P.; Pitera, K. Truck-bicycle safety: An overview of methods of study, risk factors and research needs. *Eur. Transp. Res. Rev.* **2019**, *11*, 29. [CrossRef]

17. Zhang, R.; Liu, J.; Ma, L. A typical blind area danger pre-warning method of heavy truck under turning right condition. In Proceedings of the 2015 Sixth International Conference on Intelligent Systems Design and Engineering Applications (ISDEA), Guiyang, China, 18–19 August 2015; pp. 93–96.

18. Wang, T.; Zhang, X.; Xin, Y.; Lou, J.; Yang, W. The Calculation Method and the Design of the Warning System for the Dangerous Area of the Inner Wheel difference of the Vehicle. In Proceedings of the 2021 9th International Conference on Traffic and Logistic Engineering (ICTLE), Macau, China, 9–11 August 2021; pp. 88–92.

19. Prati, G.; Puchades, V.M.; De Angelis, M.; Fraboni, F.; Pietrantoni, L. Factors contributing to bicycle–motorised vehicle collisions: A systematic literature review. *Transp. Rev.* **2018**, *38*, 184–208. [CrossRef]

20. Warner, J.; Hurwitz, D.S.; Monsere, C.M.; Fleskes, K. A simulator-based analysis of engineering treatments for right-hook bicycle crashes at signalized intersections. *Accid. Anal. Prev.* **2017**, *104*, 46–57. [CrossRef] [PubMed]

21. Alhajyaseen, W.K.; Asano, M.; Nakamura, H.; Tan, D.M. Stochastic approach for modeling the effects of intersection geometry on turning vehicle paths. *Transp. Res. Part C Emerg. Technol.* **2013**, *32*, 179–192. [CrossRef]

22. Martínez, F.; Páez, J.; Furones, A.; Sánchez, S. Pedestrian-Vehicle Accidents Reconstruction with PC-Crash®: Sensibility Analysis of Factors Variation. *Transp. Res. Procedia* **2016**, *18*, 115–121. [CrossRef]

23. Peng, Y.; Li, R.; Li, G.B.; Yang, X.M.; Zhou, D. Method for investigation of child occupant impact dynamics based on real-world accident. *Int. J. Automot. Technol.* **2015**, *16*, 791–797. [CrossRef]

24. Yuan, Q.; Li, Y.; Liao, Y.; Tang, S. Study of Correlation between Driver Emergency Measures and Pedestrian Injury Based on Combined Driving Simulator and Computer Simulation. *Adv. Mech. Eng.* **2015**, *5*, 171479. [CrossRef]

25. Wang, X.; Peng, Y.; Yi, S. Comparative analyses of bicyclists and motorcyclists in vehicle collisions focusing on head impact responses. *Proc. Inst. Mech. Eng. Part H J. Eng. Med.* **2017**, *231*, 997–1011. [CrossRef] [PubMed]

26. Seyedi, M.; Jung, S.; Wekezer, J. A comprehensive assessment of bus rollover crashes: Integration of multibody dynamic and finite element simulation methods. *Int. J. Crashworthiness* **2022**, *27*, 273–288. [CrossRef]

27. Yang, D.; Wu, Y.; Sun, F.; Chen, J.; Zhai, D.; Fu, C. Freeway accident detection and classification based on the multi-vehicle trajectory data and deep learning model. *Transp. Res. Part C Emerg. Technol.* **2021**, *130*, 103303. [CrossRef]

28. *CJJ37-2012*; Code for Design of Urban Road Engineering. Ministry of Housing and Urban-Rural Development (MHURD): Beijing, China, 2012.

29. *GB 10000-1988*; Human Dimensions of Chinese Adults. The State Bureau of Quality and Technical Supervision (SBQTS): Beijing, China, 1988.

30. *GB/T 17245-2004*; Inertial Parameters of Adult Human Body. Standardization Administration of China (SAC): Beijing, China, 2004.

31. Yu, Q.; Zhou, Y. Traffic safety analysis on mixed traffic flows at signalized intersection based on Haar-Adaboost algorithm and machine learning. *Saf. Sci.* **2019**, *120*, 248–253. [CrossRef]

32. Zhao, H.; Yin, Z.; Yang, G.; Che, X.; Xie, J.; Huang, W.; Wang, Z. Analysis of 121 fatal passenger car-adult pedestrian accidents in China. *J. Forensic Leg. Med.* **2014**, *27*, 76–81. [CrossRef]

33. Ahmed, S.N.; Darade, P.; Jagtap, K.; Ranjan, R. Comparative Analysis of Performance of Hydro-mechanical Steering System and Ideal Steering System of the SPT trailer. *Mater. Today Proc.* **2017**, *4*, 2525–2533. [CrossRef]

34. *GB 3565-2005*; Safety Requirements for Bicycles. General Administration of Quality Supervision, Inspection and Quarantine of the People's Republic of China (AQSIQ): Beijing, China, 2005.

35. *GB 7258-2017*; Technical Specifications for Safety of Power-Driven Vehicles Operating on Roads. State Administration for Market Regulatio (SAMR): Beijing, China, 2017.

36. *GB/T 24158-2018*; General Specifications for Electric Motorcycles and Electric Mopeds. State Administration for Market Regulation (SAMR): Beijing, China, 2018.

37. Lai, X.; Ma, C.; Hu, J.; Zhou, Q. Impact direction effect on serious-to-fatal injuries among drivers in near-side collisions according to impact location: Focus on thoracic injuries. *Accid. Anal. Prev.* **2012**, *48*, 442–450. [CrossRef]

38. Watanabe, R.; Katsuhara, T.; Miyazaki, H.; Kitagawa, Y.; Yasuki, T. Research of the Relationship of Pedestrian Injury to Collision Speed, Car-type, Impact Location and Pedestrian Sizes using Human FE model (THUMS Version 4). In Proceedings of the 56th Stapp Car Crash Conference, Savannah, GA, USA, 29–31 October 2012. [CrossRef]

39. Asadinia, N.; Khalkhali, A.; Saranjam, M.J. Sensitivity analysis and optimization for occupant safety in automotive frontal crash test. *Lat. Am. J. Solids Struct.* **2018**, *15*, 1–15. [CrossRef]

40. Charlebois, D.; Meloche, E.; Burns, P. Detection of Cyclist and Pedestrians around Heavy Commercial Vehicles. In Proceedings of the 26th International Technical Conference on the Enhanced Safety of Vehicles (ESV): Technology: Enabling a Safer Tomorrow National Highway Traffic Safety Administration (No. 19-0340), Eindhoven, The Netherlands, 6–13 June 2019.

41. *GB/T 39263-2020*; Road Vehicles—Advanced Driver Assistance Systems—Terms and Definitions. State Administration for Market Regulation (SAMR): Beijing, China, 2020.
42. *GB/T 39265-2020*; Road Vehicles—Performance Requirements and Testing Methods for Blind Spot Detection (BSD) System. State Administration for Market Regulation (SAMR): Beijing, China, 2020.